solution for uniform flow ($u/u_e = 1$), although in the latter case $v(y) \neq 0$ because of the positive pressure gradient. Figure 1 and Table 1 show the variation of the normalized velocity on the axis with the pressure gradient parameter n. The velocity on the axis vanishes for $n = 0.650$; hence this solution corresponds, at least conceptually, to the rear stagnation point found in steady wake flows.

The velocity profiles for various values of n are shown in Fig. 2. It is noteworthy that the present solutions for separated flow ($\frac{1}{2} < n < 0.648$) yield much larger back-flow velocities than do the two-dimensional solutions[3] and are apparently due to a "squeezing" effect that is a result of the axisymmetric geometry.

References

[1] Stewartson, K., "Further solutions of the Falkner-Skan equation," Proc. Cambridge Phil. Soc. **50**, 454–465 (1954).

[2] Lees, L. and Reeves, B. L., "Supersonic separated and reattaching laminar flows: I. General theory and application to adiabatic boundary layer-shock wave interactions," AIAA Preprint 64-4 (January 1964).

[3] Kennedy, E. D., "Wake-like solutions of the laminar boundary-layer equations," AIAA J. **2**, 225–231 (1964).

[4] Chapman, D. R., "Laminar mixing of a compressible fluid," NACA Rept. 958 (1950).

[5] Schlichting, H., *Boundary Layer Theory* (McGraw-Hill Book Co., Inc., New York, 1960), Chap. 10.

Analysis of MHD Channel Entrance Flows Using the Momentum Integral Method

W. Craig Moffatt*

Massachusetts Institute of Technology, Cambridge, Mass.

THE use of integral methods for solution of the laminar boundary-layer equations is a widely accepted technique in ordinary hydrodynamics. In general, solutions are found by integrating the equations in two steps: first in the direction normal to the wall, using an assumed velocity distribution, and then in the flow direction, where a new dependent variable, the boundary-layer "thickness," arises as a result of the first integration. Such methods are of limited usefulness, since they give no indication of the detailed nature of the flow; however, they have proved to be of considerable value in assessing such effects as skin friction and heat transfer, the solutions for which prove to be relatively insensitive to the particular profiles assumed.

Several authors have attempted to apply integral methods to MHD flows, using simple parabolic[1, 2] or Karman-Pohlhausen[3] velocity distributions. Although these solutions show the correct qualitative behavior (eg., the asymptotic approach to a constant boundary-layer thickness when the magnetic field is applied normal to the surface and the flow), the quantitative results are suspect, primarily because of the assumed parabolic profile.

The success of such profiles in ordinary hydrodynamic entrance flows (e.g., Sparrow[4]) probably can be attributed to the fact that the asymptotic solution far from the channel entrance (plane Poiseuille flow) can be found exactly and yields a parabolic distribution. Correspondingly, it would be expected that the logical distribution to use for MHD entrance flows would be the asymptotic solution for the magnetic case, i.e., Hartmann flow.

Received April 15, 1964. This work was performed under the auspices of Project SQUID, Nonr-3623(S-2). The facilities of the Massachusetts Institute of Technology Computation Center were used for the numerical calculations.

* Assistant Professor of Mechanical Engineering. Member AIAA.

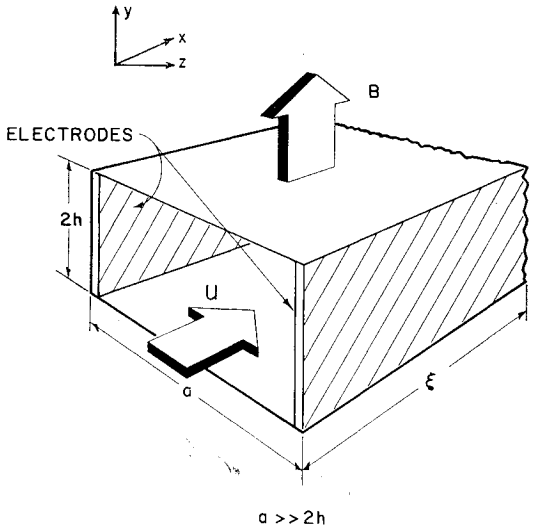

Fig. 1. Schematic diagram of entrace to MHD channel. The value of $K = E/UB$ is determined by the nature of the external electrical connection between the electrodes.

Several authors have treated these flows using other techniques. For example, Roidt and Cess,[5] following a method developed by Schlichting for nonmagnetic flow, divided the entrance region into two sections, an upstream section where the solution was patterned after the Blasius series solution, and a downstream section where the velocity was expressed as the fully developed profile plus a deviation velocity. On the other hand, Shohet et al.[6] solved the entrance region problem numerically by writing the momentum and continuity equations in a stable finite difference form. The purpose of this note is to present the results of a solution based on the momentum integral method using an assumed Hartmann-like velocity distribution.

For fully developed, incompressible, steady flow of an electrically conducting fluid at low magnetic Reynolds number in the channel shown in Fig. 1, the x-momentum equation becomes

$$(dp/dx) + jB - \mu(d^2u/dy^2) = 0 \tag{1}$$

where, in the absence of Hall effects,

$$j = \sigma(uB - E) \tag{2}$$

In these equations, j is the current density, σ the electrical conductivity of the fluid, and B and E the imposed magnetic and electric field strengths, respectively. These equations can be readily solved (see, for example, Ref. 7) to yield

$$u = \left(\frac{E}{B} - \frac{dp/dx}{\sigma B^2}\right)\left[1 - \frac{\cosh\{M(1 - y/h)\}}{\cosh M}\right] \tag{3}$$

where $M = Bh(\sigma/\mu)^{1/2}$ is the Hartmann number. Since the first bracketed term in Eq. (3) is constant for fully developed flow, a dimensionless velocity distribution

$$\frac{u}{u_c} = \frac{\cosh M - \cosh\{M(1 - y/h)\}}{\cosh M - 1} \tag{4}$$

can be formed, where u_c is the velocity at the center of the channel.

The momentum and continuity equations for boundary layers on the nonconducting walls of the channel shown in Fig. 1 may be written as

$$u\frac{\partial u}{\partial x} + v\frac{\partial u}{\partial y} = -\frac{1}{\rho}\frac{\partial p}{\partial x} - \frac{jB}{\rho} + \frac{\mu}{\rho}\frac{\partial^2 u}{\partial y^2} \tag{5}$$

$$(\partial u/\partial x) + (\partial v/\partial y) = 0 \tag{6}$$

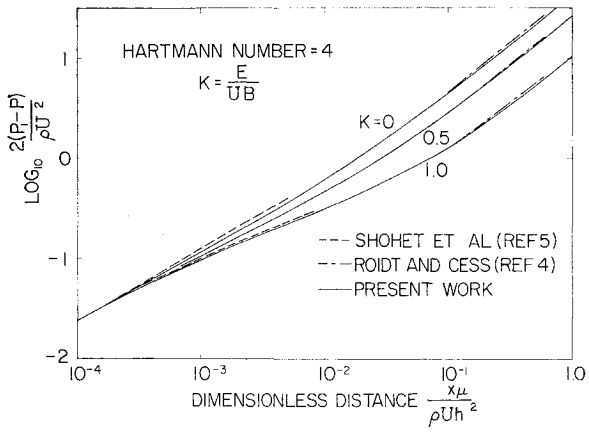

Fig. 2. Pressure distribution in entrance region of channel for several operating conditions at $M = 4$.

Following the standard integral procedure (e.g., Ref. 1), Eqs. (5) and (6) may be integrated in the y direction between the limits 0 and δ, where δ is the boundary-layer thickness (i.e., the value of y such that, for $y \geq \delta$, $u = u_c$). The resulting momentum equation is

$$u_c^2 \frac{d\theta}{dx} + (u_c\delta^* + 2u_c\theta)\frac{du_c}{dx} = \frac{-\sigma u_c B^2 \delta^*}{\rho} - \frac{\mu}{\rho}\int_0^\delta \frac{\partial^2 u}{\partial y^2}\,dy \tag{7}$$

where δ^*, the displacement thickness, is defined as

$$\delta^* \equiv \int_0^\delta \left(1 - \frac{u}{u_c}\right) dy \tag{8}$$

and θ, the momentum thickness, as

$$\theta \equiv \int_0^\delta \frac{u}{u_c}\left(1 - \frac{u}{u_c}\right) dy \tag{9}$$

Similarly, the continuity equation becomes

$$\delta^* + h(U/u_c - 1) = 0 \tag{10}$$

where U is the assumed uniform axial velocity at the inlet to the channel. Note that, in the entrance region of the channel, u_c is a function of x.

To obtain a solution to Eq. (7), δ^* and θ must be found from Eqs. (8) and (9) based on an assumed distribution of u/u_c with y. By virtue of the reasoning outlined in the foregoing, a relation of the form

$$\frac{u}{u_c} = \frac{\cosh M - \cosh\{M(1 - y/\delta)\}}{\cosh M - 1} \tag{11}$$

is appropriate. This equation is identical with Eq. (4), except that h has been replaced by δ. This profile satisfies the boundary conditions:

$$y = 0: \qquad u = 0$$

$$y = \delta: \qquad u = u_c$$

$$du/dy = 0$$

It does not, however, satisfy the condition $(d^2u/dy^2)_{y=\delta} = 0$ For the limiting case of very small Hartmann numbers, it can be easily shown by expansion of the hyperbolic cosine terms that Eq. (11) reduces to the parabolic form used by Sparrow.[4]

Substitution of Eq. (11) into Eqs. (8) and (9) yields the results

$$\delta^* = K_1\delta \tag{12}$$

$$\theta = K_2\delta \tag{13}$$

where

$$K_1 = \frac{1}{M}\left(\frac{\sinh M - M}{\cosh M - 1}\right) \tag{14}$$

$$K_2 = \frac{1}{\cosh M - 1}\left[\cosh M - \frac{\sinh M}{M} - \frac{\cosh^2 M - (2/M)\cosh M \sinh M + \frac{1}{2} + (\sinh 2M/4M)}{\cosh M - 1}\right] \tag{15}$$

Furthermore, the last term on the right-hand side of Eq. (7) becomes

$$\frac{\mu}{\rho}\int_0^\delta \frac{\partial^2 u}{\partial y^2}\,dy = -\frac{K_3 u_c \mu}{\rho\delta} \tag{16}$$

where

$$K_3 = M \sinh M/(\cosh M - 1) \tag{17}$$

From Eq. (12) and the continuity relation, Eq. (10), the boundary-layer thickness becomes

$$\delta = (h/K_1)(1 - U/u_c) \tag{18}$$

Substitution of Eqs. (12–18) into the momentum equation (7) yields, after rearrangement,

$$\frac{du_c'}{d\xi} = \frac{K_3K_1u_c'^2 - (u_c' - 1)^2M^2}{\{(K_2/K_1)(u_c' - 1) + [1 + (2K_2/K_1)](u_c' - 1)^2\}} \tag{19}$$

where

$$u_c' = u_c/U \qquad \xi = x\mu/\rho h^2 U$$

The pressure distribution in the channel entrance region can be found by writing the momentum equation for the free-stream as

$$dp/dx = -\rho u_c(du_c/dx) - j_c B \tag{20}$$

From Eq. (2), it is evident that

$$j_c = \sigma(u_c B - E)$$

$$= \sigma u_c B[1 - (K/u_c')]$$

where $K = E/UB$. The physical significance of the quantity K/u_c' is as follows:

$K/u_c' = 0$	electrodes short-circuited
$0 < K/u_c' < 1$	channel acts as a generator
$K/u_c' = 1$	electrodes open-circuited
$K/u_c' > 1$	channel acts as a pump

In dimensionless form, Eq. (20) becomes

$$dp'/d\xi = 2u_c'(du_c'/d\xi) + 2M^2(u_c' - K) \tag{21}$$

where $p' = (P_1 - P)/\frac{1}{2}\rho U^2$, P is the pressure at any value of ξ, and P_1 is the pressure at $\xi = 0$.

Equations (19) and (21) were solved numerically, and the results are shown in Fig. 2 for several values of K when $M = 4$. The agreement between the pressure distributions, found from the simple integral method and the more complex techniques of Refs. 5 and 6, is seen to be remarkably good.

In order to ascertain the effect of the assumed boundary-layer velocity profile on the entrance region pressure distribution, the calculations were repeated using the parabolic profile of Refs. 1 and 2. It was found that, close to the channel entrance, the results were in substantial agreement with those of Shohet et al.; however, at the large values of ξ, discrepancies as large as 20% were encountered. This result is not surprising because, near the entrance to the channel, the ratio of magnetic to inertia forces ($M^2\xi$) is small, and the boundary-layer growth will correspond to that for ordinary viscous flows. Thus, for $M^2\xi < 1$, the parabolic profile should yield acceptable results. However, further down the channel ($M^2\xi > 1$), the boundary-layer growth is governed primarily by magnetic and viscous forces, and in this region the velocity distribution in the layer is more nearly like the flat Hartmann-

like profile of Eq. (11) than a parabola. It is for this reason that the present analysis would seem to be appropriate for those cases where magnetic effects are important over a significant portion of the channel length.

References

[1] Moffatt, W. C., "Boundary layer effects in magnetohydrodynamic flows," Magnetogasdynamics Lab. Rept. 61-4, Dept. of Mechanical Engineering, Massachusetts Institute of Technology, Cambridge, Mass. (May 1961); also Armed Services Technical Information Agency Doc. AD-259490 (May 1961).

[2] Maciulaitis, A. and Loeffler, A. L., "A theoretical investigation of MHD channel entrance flows," American Physical Society Paper E2 (November 1963).

[3] Heywood, J. B., "Magnetogasdynamic laminar boundary layer and channel flow phenomena," S. M. Thesis, Dept. of Mechanical Engineering, Massachusetts Intitute of Technology, Cambridge, Mass. (May 1962).

[4] Sparrow, E., "Analysis of laminar forced-convection heat transfer in entrance region of flat rectangular ducts," NACA TN3331 (January 1955).

[5] Roidt, M. and Cess, R. D., "An approximate analysis of laminar magnetohydrodynamic flow in the entrance region of a flat duct," J. Appl. Mech. **19**, 171–176 (1962).

[6] Shohet, J. L., Osterle, J. F., and Young, F. J., "Velocity and temperature profiles in laminar magnetohydrodynamic flow in the entrance region of a plane channel," Phys. Fluids **5**, 545–549 (1962).

[7] Yoler, Y. A., "A review of magnetohydrodynamics," *Plasma Physics*, edited by J. E. Durmmond (McGraw-Hill Book Co., Inc., New York, 1961), p. 193.

Equilibrium Electron Density on Mars

EDWARD D. SHANE*
Avco Corporation, Wilmington, Mass.

IN order to investigate the possibility of communication blackout during entry into the Martian atmosphere, it is necessary to make estimates of the expected electron concentration. The following contains thermochemical equilibrium values of electron concentration corresponding to five models[1, 2] of the Martian atmosphere as a function of temperature and density. The results show that at a given temperature and density the electron concentration on Mars will be less than that on Earth, and that this is most evident at low temperatures and high densities.

The five atmospheric models considered are shown in Table 1. Figures 1–5 show equilibrium electron concentration for the various atmospheric models as a function of temperature and density. Figures 6 and 7 show electron concentration for all 5 models and for the Earth's atmosphere[3] as a function of density at 2000° and 5000°K, respectively.

In all of the atmospheres in which both nitrogen and oxygen are assumed present, the principle source of electrons is due to ionized NO at 2000° and 3500°K and to both NO and C at 5000°K. For the atmospheric model in which nitrogen is assumed absent, the electron density is essentially due to ionized O_2 at the lower temperatures and to O_2, O, C, and CO at 5000°.

Table 1 Mars atmospheric models

Atmospheric model	Percent composition		
	CO_2	A	N_2
Kaplan[1]			
1	65	35	0
2	43	32	25
3	11	13	76
Spiegel[2]			
4	7.2	6.0	86.8
5	0.7	0.6	98.7

Received March 12, 1964.

* Associate Engineer, Research and Advanced Development Division.

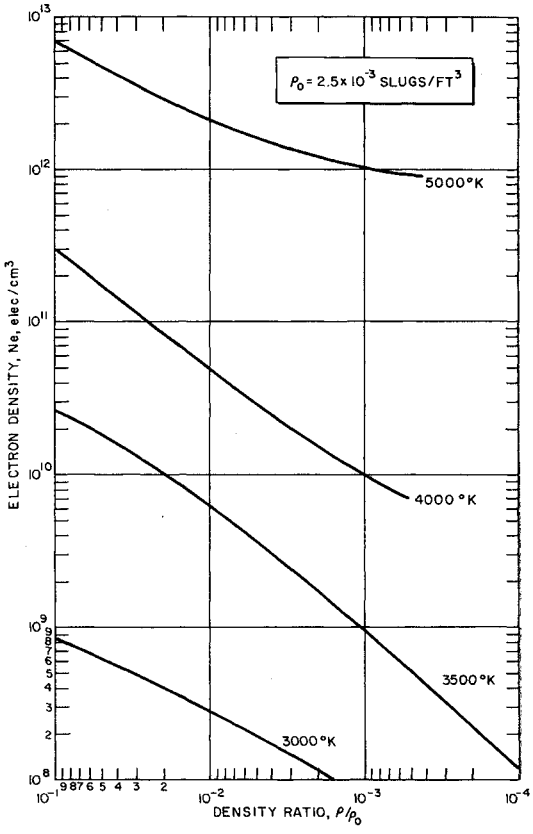

Fig. 1 Equilibrium electron density, 65% CO_2, 35% A.

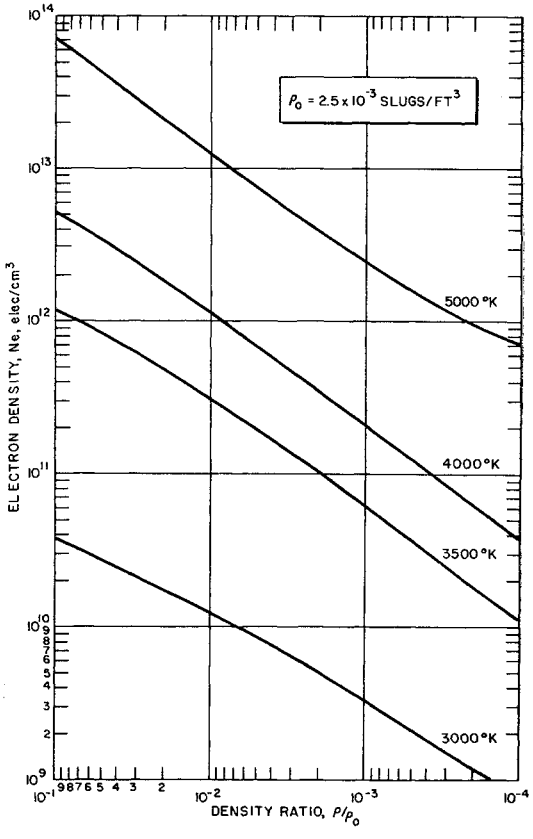

Fig. 2 Equilibrium electron density, 43% CO_2, 32% A, 25% N_2.